Journal of Porous Media, 22(11):1411–1422 (2019)

COMBINED EFFECTS OF MECHANICAL VIBRATION AND MAGNETIC FIELD ON THE ONSET OF BUOYANCY-DRIVEN CONVECTION IN AN ANISOTROPIC POROUS MODULE

A. Purusothaman[1,*] *& Ali J. Chamkha*[2,3]

[1]*Department of Mathematics, National Institute of Technology, Tiruchirappalli 620015, India*
[2]*Mechanical Engineering Department, Prince Mohammad Bin Fahd University, Al-Khobar 31952, Saudi Arabia*
[3]*RAK Research and Innovation Center, American University of Ras Al Khaimah, United Arab Emirates*

*Address all correspondence to: A. Purusothaman, Department of Mathematics, National Institute of Technology, Tiruchirappalli 620015, India; Tel.: +91-9944317732; Fax: +91-431-2500133, E-mail: abipurus@gmail.com

Original Manuscript Submitted: 7/26/2018; Final Draft Received: 12/27/2018

The combined impacts of mechanical variation and the applied magnetic field on the onset of convection in an infinite flat liquid permeated anisotropic porous module are investigated subject to an adverse temperature gradient. The Brinkman model is taken to describe the flow momentum in the porous module, and the Boussinesq approximation is implicated in the field of buoyancy-driven flow. Floquet theory is applied to govern the onset condition within the framework of linear stability analysis. The present study is focused on the small amplitude gravity vibration, and the thresholds are found using Mathieu's functions and stability charts. Specific attention is paid to examine the effects on anisotropies in permeability and thermal conductivity of the porous module along the transverse direction. The emerging instabilities of synchronous and subharmonic modes and the exact point of the transition between them are examined for the control parameters. The applied magnetic field is more effective in stabilizing the system subject to gravity modulation than the system subject to gravity modulation alone. The findings of this analysis will give additional knowledge in controlling convective streams in designing highly perfect crystals or materials with improved mechanical properties.

KEY WORDS: *convection, stability, gravity vibration, porous module, magnetic field*

1. INTRODUCTION

Free convection in a fluid-saturated porous module has received considerable attention in recent years due to its numerous applications in different fields such as nuclear waste repository, solidification of molten alloys, oil reservoir modeling, and geothermal fields, to name a few. Crystal growth is an interdisciplinary area which requires a thorough knowledge of hydrodynamics associated with heat transfer through a porous module. The primary goal of a crystal grower is to manufacture highly perfect crystals or materials required for modern technology which are free from structural nonuniformities. Thermal convection in a horizontal fluid-saturated porous module was first investigated by Horton and Rogers, Jr. (1945) and individually by Lapwood (1948) using linear stability analysis. Their results were later confirmed experimentally by Elder (1967) and Katto and Masuoka (1967). Comprehensive reviews of literature and the fundamental applications of heat transfer in the porous module were well documented by Ingham and Pop (1998), Vafai (2005), and Nield and Bejan (2006).

1091–028X/19/$35.00

NOMENCLATURE

$\vec{B}$	magnetic field induction vector
B_0	external magnetic field
b_*	vibration amplitude
Da	Darcy number, K_{z*}/H_*^2
$\vec{F}$	Lorentz force
Fr	Froude number, $\lambda_{z*}^2/g_*H_*^3$
$\vec{g_*}$	gravitational acceleration
H_*	height of the porous module
Ha	Hartmann number
$\vec{J_*}$	electric current density
$\overline{\overline{K}}_*$	permeability tensor, $K_{x*}(\vec{i}\vec{i}+\vec{j}\vec{j})+K_{z*}\vec{k}\vec{k}$
L_*	length of the porous module
p	pressure
Pr	Prandtl number
R	Rayleigh number, $\beta_*\Delta T_C g_* K_{z*} H_*/\nu_*\lambda_{z*}$
s	wave number
T	temperature, $(T_*-T_C)/(T_H-T_C)$
t	time
u	horizontal x component of the filtration velocity
v	horizontal y component of the filtration velocity
$\vec{V}$	filtration velocity vector, $u\vec{i}+v\vec{j}+w\vec{k}$
$\vec{V_1}$	anisotropy modified velocity vector, $(u/\xi)\vec{i}+(v/\xi)\vec{j}+w\vec{k}$
Va	Vadasz number, ϕ Pr/Da
w	vertical z component of the filtration velocity
x	horizontal length coordinate
y	horizontal width coordinate
z	vertical coordinate

Greek Symbols

α	parameter related to the wave number, s^2/π^2
β_*	thermal expansion coefficient
γ	Va/π^2
δ	amplitude, $\kappa Fr\Omega^2$
ΔT_C	characteristic temperature difference
κ	b_*/H_*
$\overline{\overline{\lambda}}_*$	thermal diffusivity tensor, $\lambda_{x*}(\vec{i}\vec{i}+\vec{j}\vec{j})+\lambda_{z*}\vec{k}\vec{k}$
μ_*	dynamic viscosity
μ_{e*}	effective dynamic viscosity
$\overline{\mu}$	μ_{e*}/μ_*
ν_*	kinematic viscosity
ξ	mechanical anisotropy parameter, K_{x*}/K_{z*}
η	thermal anisotropy parameter, $\lambda_{x*}/\lambda_{z*}$
ς	scaled exponent, equals $\sigma/\sqrt{-a}$
ρ_*	fluid density
σ	Mathieu exponent
σ_{m*}	electrical conductivity
ϕ	porosity
ω_*	vibration frequency
Ω	scaled vibration frequency, $\omega_* H_*^2/\lambda_{z*}$

Subscripts

$*$	dimensional quantity
c	characteristic
cr	critical
C	cold wall
H	hot wall
o	unmodulated quantity

External regulation of convection is important for either enhancing or diminishing heat transfer in the physical systems. Several techniques have been used for controlling the convective instability of such systems. Gravity, rotational, thermal modulation, and magnetic field are a few of them being adopted to reach this objective. Modulation of the gravity field introduces a variable body force, usually gravity fluctuating with time in the presence of density gradients. Its significance on thermal convection depends on the direction of the body force relative to the thermal gradient. Gershuni et al. (1970) and Gresho and Sani (1970) first examined the g-jitter effect in a differentially heated fluid-filled module. They found that the undesirable buoyancy-driven flow in a differentially heated fluid layer is stabilized by the appropriate vertical vibrations. Further, the stability solution of a fluid-drenched porous module depending on small amplitude vertical vibration was investigated by Malashetty and Padmavathi (1997). They noticed that the imposed vibration considerably influences the stability limits of the system.

Govender (2005) discussed the g-jitter effect on the onset of convection in a differentially heated homogeneous porous module. He predicted the exact changeover point from the synchronous to the subharmonic solution using

Mathieu's stability charts. Saravanan and Purusothaman (2009) later confirmed Govender's results and also examined the effects of anisotropy parameters of the porous module subject to vertical vibration using the Brinkman model. Thermal convection instability in a mushy module depending on gravity modulation has been examined by Srivastava and Bhadauria (2011). They discussed the influence of pertinent parameters on the stability of the module. The fundamental researches on the stability of a rotating porous module have significantly augmented due to its diverse industrial requirements. The detailed discussions and its applications on thermal convection in a rotating porous module were explored by Govender (2006) and Malashetty and Swamy (2010).

The topic of thermal stability in a fluid-drenched porous module induced by vibrating forces such as the modulated gravity forces, vibrating wall temperatures, or the combination of these two under the presence of a magnetic field has been investigated for the past few decades due to its noteworthy applications in different fields and industries. The effect of magnetic field modulation on a horizontal magnetic fluid-filled module was studied by Aniss et al. (2001). They exhibited the possibility of stabilizing and destabilizing effects on the onset of convection with a suitable choice of the proportion of the magnetic and oscillating forces. Li (2001) examined the linear stability analysis of convective instability in a differentially heated fluid module subject to an externally imposed magnetic field. Also, Mahabaleswar (2007) inspected the combined effect of magnetic field and thermal modulation on the onset of convection in a weak electrically conducting micropolar liquid-filled module. The problem was further investigated with an electrically conducting fluid-drenched porous module by Bhadauria (2008). Siddheshwar et al. (2012) examined the weakly nonlinear stability analysis of magneto convection in an electrically conducting Newtonian fluid-filled module subjected to thermal or gravity vibration. It was clearly revealed from these surveys that the imposed external magnetic force is found to stabilize the system subject to oscillating forces. Recently, the natural convection heat transfer in nanofluid was investigated subject to applied magnetic field by many researchers, for instance, Purusothaman et al. (2016a), Chamkha et al. (2017, 2018), and Rashad et al. (2018). It was found that the heat transfer rate amplifies with increasing the nanoparticle solid volume fraction; however, the convection currents are highly suppressed by the enforced magnetic field.

Therefore, the main objective of the present study is to investigate the combined impacts of gravity variation and magnetic field on the stability of convective flow through a liquid-saturated anisotropic porous module. A linear stability analysis is made to show how the combined effect of gravity modulation and applied horizontal magnetic field can significantly affect the stability limits of the system. The Brinkman model is taken to describe the flow momentum in the porous module. Specific attention is paid to analysis of the effects on anisotropies in permeability and thermal conductivity of the porous module along the transverse direction. The findings of this analysis will give additional knowledge in controlling convective streams in designing highly perfect crystals or materials with improved mechanical properties.

2. MATHEMATICAL FORMULATION

The geometry and the coordinate system are schematically shown in Fig. 1. An infinite horizontal fluid-saturated sparsely packed anisotropic porous module confined between the surfaces $z_* = 0$ and $z_* = H^*$ is considered. A homogeneous magnetic field expressed by $\vec{B}(B_0, 0, 0)$ is imposed parallel to the x_* axis. The module is heated from below and is depending on the low-amplitude vibration in the vertical direction. Brinkman's law is used and the convective terms are neglected as we deal with a quiescent initial state. The system of dimensional equations describing the above coordination under the hypothesis of Boussinesq are given by the following (Purusothaman, 2018; Purusothaman et al., 2016b),

$$\nabla_* \cdot \vec{V}_* = 0 \tag{1}$$

$$\frac{\rho_{c^*}}{\phi}\frac{\partial \vec{V}_*}{\partial t_*} = -\nabla_* p_* - \frac{\mu_*}{\overline{\overline{K}}_*}\vec{V}_* + \mu_{e^*}\nabla_*^2\vec{V}_* - (\rho_* - \rho_{c^*})[g_* + b_* w_*^2 \sin(w_* t_*)]\vec{k} + \vec{J}_* \times \vec{B} \tag{2}$$

$$\frac{\partial T_*}{\partial t_*} + \vec{V}_* \cdot \nabla_* T_* = \nabla_* \cdot (\overline{\overline{\lambda}}_* \cdot \nabla_* T_*) \tag{3}$$

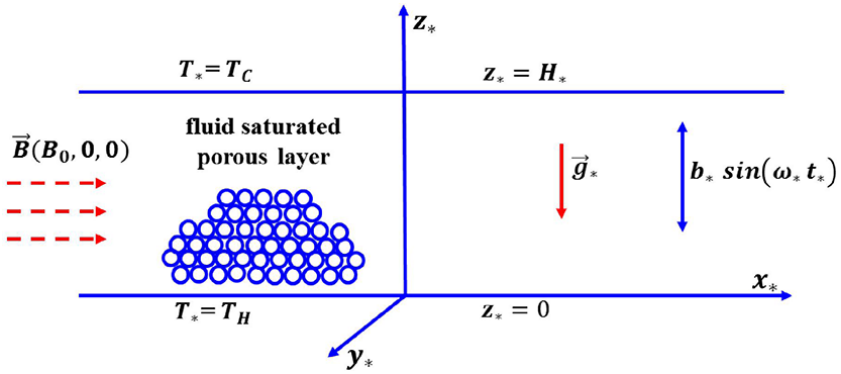

FIG. 1: Schematic of a differentially heated porous module subjected to the combined action of gravity modulation and applied magnetic field

$$\nabla.\vec{J}_* = 0 \tag{4}$$

$$\vec{J}_* = \sigma_{m*}(\vec{V}_* \times \vec{B}) \tag{5}$$

Further, this research is principally focused on two-dimensional disturbances in the x_* and z_* directions. Hence, the component of the Lorentz force is assumed to be systematically negligible in the y_* direction. The Lorentz force $\vec{J}_* \times \vec{B}$ then reduces to $-\sigma_{m*}B_0^2 w_* \vec{k}$. The physical framework is nondimensionalized using the following parameters:

$$\begin{aligned}
&(x_*, y_*, z_*) = H_*(x, y, z), \quad (u_*, v_*, w_*) = \frac{\lambda_{z^*}}{H_*}(u, v, w), \quad t_* = \frac{H_*^2}{\lambda_{z^*}}t, \\
&p_* = \left(\frac{\mu_* \lambda_{z^*}}{K_{z^*}}\right) p, \quad (T_* - T_C) = \triangle T_C T = (T_H - T_C)T, \quad \rho_* = \rho_{c^*}(1 - \beta_* \triangle T_C T), \\
&\mu_* = \nu_* \rho_{c^*}, \quad R = \beta_* \triangle T_C g_* K_{z^*} H_* / \nu_* \lambda_z, \quad \mathrm{Ha} = B_0 H_* \sqrt{\sigma_{m*}/\mu_*}
\end{aligned} \tag{6}$$

and express Eqs. (1)–(3) in non-dimensional form as

$$\nabla \cdot \vec{V} = 0 \tag{7}$$

$$\frac{1}{\mathrm{Va}}\frac{\partial \vec{V}}{\partial t} + \vec{V}_1 - \mathrm{Da}\nabla^2 \vec{V} = -\nabla p + R\left[1 + \delta \sin(\Omega t)\right] T\vec{k} - \mathrm{Ha}^2\,\mathrm{Da}\, w\vec{k} \tag{8}$$

$$\frac{\partial T}{\partial t} + \vec{V} \cdot \nabla T = \left(\eta \nabla_H^2 + \frac{\partial^2}{\partial z^2}\right) T \tag{9}$$

where $\Omega = \omega_* H_*^2/\lambda_z$ denotes the scaled frequency, $\delta = \kappa \mathrm{Fr}\Omega^2$ denotes the amplitude, $\kappa = b_*/H_*$, and $\mathrm{Fr} = \lambda_{z^*}^2/(g_* H_*^3)$ denote the modified Froude number. The parameter Va is the Vadasz number and is defined as

$$\mathrm{Va} = \frac{\phi \mathrm{Pr}}{\mathrm{Da}} \tag{10}$$

where $\mathrm{Pr} = \nu_*/\lambda_{z^*}$ is the Prandtl number and $\mathrm{Da} = K_{z^*}/H_*^2$ is the Darcy number. The boundaries are presumed to be horizontal and stress-free, that is, $w = 0$ and $(\partial u/\partial z) = (\partial v/\partial z) = 0$. The thermal boundary conditions are $T = 1$ at $z = 0$ and $T = 0$ at $z = 1$. The perturbations around the basic state solution are assumed in the form $V = V_B + V'$ and $T = T_B + T'$, where $V_B = 0$ and $T_B = 1 - z$. Replacing these in Eqs. (7)–(9), excluding the pressure by applying the curl operator twice in Eq. (8) and projecting it on the z direction, the equations describe the perturbations as

$$\begin{aligned}
&\left(\frac{1}{\mathrm{Va}}\frac{\partial}{\partial t}\right)\nabla^2 w' + \nabla_H^2 w' + \frac{1}{\xi}\frac{\partial^2 w'}{\partial z^2} - \mathrm{Da}\,\nabla^2\nabla^2 w' - R\left[1 + \delta \sin(\Omega t)\right]\nabla_H^2 T' \\
&\qquad + \mathrm{Ha}^2\,\mathrm{Da}\,\nabla_H^2 w' = 0
\end{aligned} \tag{11}$$

$$\left[\frac{\partial}{\partial t}-\left(\eta\nabla_H^2+\frac{\partial^2}{\partial z^2}\right)\right]T'-w'=0 \tag{12}$$

where w' is the vertical component of the perturbed velocity. The appropriate boundary conditions are $w'=(\partial^2 w')/(\partial z^2)=T'=0$ at $z=0$ and $z=1$. We eliminate w' from Eqs. (11) and (12) to obtain a single equation for the temperature perturbation in the form

$$\begin{aligned}&\left(\frac{1}{\mathrm{Va}}\frac{\partial}{\partial t}\right)\nabla^2\left[\frac{\partial}{\partial t}-\left(\eta\nabla_H^2+\frac{\partial^2}{\partial z^2}\right)\right]T'+\nabla_H^2\left[\frac{\partial}{\partial t}-\left(\eta\nabla_H^2+\frac{\partial^2}{\partial z^2}\right)\right]T'\\&+\frac{1}{\xi}\frac{\partial^2}{\partial z^2}\left[\frac{\partial}{\partial t}-\left(\eta\nabla_H^2+\frac{\partial^2}{\partial z^2}\right)\right]T'-\mathrm{Da}\,\nabla^2\nabla^2\left[\frac{\partial}{\partial t}-\left(\eta\nabla_H^2+\frac{\partial^2}{\partial z^2}\right)\right]T'\\&-R\left[1+\delta\sin(\Omega t)\right]\nabla_H^2T'+\mathrm{Ha}^2\,\mathrm{Da}\,\nabla_H^2\left[\frac{\partial}{\partial t}-\left(\eta\nabla_H^2+\frac{\partial^2}{\partial z^2}\right)\right]T'=0\end{aligned} \tag{13}$$

Assuming an expansion into normal modes in the x and y directions and a time-dependent amplitude $\theta(t)$ of the form

$$T'=\theta(t)\exp\left[i(s_x x+s_y y)\right]\sin(\pi z) \tag{14}$$

where $s^2=s_x^2+s_y^2$. Substituting Eq. (14) into Eq. (13) provides an ordinary differential equation for the amplitude $\theta(t)$

$$\frac{d^2\theta}{dt^2}+2p\frac{d\theta}{dt}-F(\alpha)\gamma\left[(\tilde{R}-\tilde{R}_0)+\tilde{R}\delta\sin(\Omega t)\right]\theta=0 \tag{15}$$

where $2p=\pi^2\left(\eta\alpha+1+\gamma\left\{[(\xi\alpha+1)/\xi(\alpha+1)]+\mathrm{Da}\,\pi^2(\alpha+1)+\mathrm{Ha}^2\mathrm{Da}\,[\alpha/(\alpha+1)]\right\}\right)$, $\alpha=s^2/\pi^2$, $\gamma=\mathrm{Va}/\pi^2$, $\tilde{R}=R/\pi^2$, $F(\alpha)=\pi^4\alpha/(\alpha+1)$, and $\tilde{R}_0$ is the unmodulated Rayleigh number defined as $\tilde{R}_0=[(\alpha+1)^2/\alpha]\times\left\{[(\xi\alpha+1)(\eta\alpha+1)]/[\xi(\alpha+1)^2]+\mathrm{Da}\,\pi^2(\eta\alpha+1)+\mathrm{Ha}^2\,\mathrm{Da}\,[\alpha(\eta\alpha+1)/(\alpha+1)^2]\right\}$. Using the transformation $t=(\pi/2-2\tau)/\Omega$, Eq. (15) can be expressed in the canonical form of Mathieu's equation [see McLachlan (1964)] as

$$\frac{d^2X}{d\tau^2}+[a-2q\cos(2\tau)]\,X=0 \tag{16}$$

The solution to the above equation is of the form $X=\theta(\tau)e^{\sigma\tau}$, where $\theta(\tau)$ is a periodic function with a period of π or 2π and σ is a characteristic exponent which is a complex number and is a function of a and q. Here the definitions for a, q, and σ are obtained upon transforming Eq. (15) to the canonical form and are given by

$$\frac{2}{\sqrt{-a}}=\frac{\Omega}{\left[F(\alpha)\gamma(\tilde{R}-\zeta)\right]^{1/2}} \tag{17}$$

$$\frac{1}{2}q=\frac{F(\alpha)\gamma\tilde{R}\delta}{\Omega^2}=F(\alpha)\gamma\tilde{R}\kappa\,\mathrm{Fr} \tag{18}$$

$$\sigma=-2p/\Omega \tag{19}$$

where ζ is a parameter defined as

$$\zeta=-\tilde{R}_0\frac{\left\{\eta\alpha+1-\gamma\left[\frac{(\xi\alpha+1)}{\xi(\alpha+1)}+\mathrm{Da}\,\pi^2(\alpha+1)+\mathrm{Ha}^2\,\mathrm{Da}\,\frac{\alpha}{(\alpha+1)}\right]\right\}^2}{4\gamma(\alpha+1)\left[\frac{(\xi\alpha+1)(\eta\alpha+1)}{\xi(\alpha+1)^2}+\mathrm{Da}\,\pi^2(\eta\alpha+1)+\mathrm{Ha}^2\mathrm{Da}\,\alpha\frac{(\eta\alpha+1)}{(\alpha+1)^2}\right]} \tag{20}$$

3. SOLUTION PROCEDURE

The characteristic exponent with the largest $\mathrm{Re}(\sigma)$ governs the stability of the system. The disturbances intensify if $\mathrm{Re}(\sigma) \geq 0$ and decline if $\mathrm{Re}(\sigma) \leq 0$. If $\mathrm{Re}(\sigma) = 0$, the solution to Eq. (16) is defined in terms of Mathieu's functions $ce_n(a, q)$ and $se_m(a, q)$, $n = 0, 1, 2, \ldots$, $m = 1, 2, \ldots$. Detailed discussion on the properties of these functions can be found in the book by McLachlan (1964). Figure 2(a) displays the graphs of ce_0, se_1, and ce_1, which separate the stable and unstable solutions. Here, the q values are presumed to be small, and therefore the lower order function of ce_0, se_1, and ce_1 is enough for this investigation. The region below the curve ce_0 and the region bounded between the curves se_1 and ce_1 stand for the unstable zones.

A graph of $q/2$ against $2/\sqrt{-a}$, for different values of the modified characteristic exponent $\varsigma = \sigma/\sqrt{-a}$, is displayed in Fig. 2(b) for small values of q. In Fig. 2(b), $\varsigma = 0$ denotes Mathieu's function represented by the curves for ce_0 and se_1. Now, the relation for the characteristic Rayleigh number in terms of the parameter ς, by replacing $\varsigma = \sigma/\sqrt{-a}$ in Eq. (17), is presented as follows:

$$\tilde{R} = \zeta + \frac{(\tilde{R}_0 - \zeta)}{\varsigma^2} \tag{21}$$

Figure 2(b) together with Eqs. (17)–(21) is used to compute the $\tilde{R}_{cr}$ and α_{cr} in terms of the frequency Ω and the parameters $(\kappa \mathrm{Fr})$ and γ. The characteristic Rayleigh number against the frequency for particular values of α are calculated in the following way: (i) choose a value of ς, (ii) calculate $\tilde{R}$ using Eq. (21), (iii) calculate the value for $q/2$ using Eq. (18), (iv) read $2/\sqrt{-a}$ from Fig. 2(b), and (v) calculate Ω from Eq. (17). The R_{cr} is then attained by minimizing R_c over α.

In order to check the accurateness of the current work, the present results are validated corresponding to a fluid-drenched porous module of Darcian nature and the absence of magnetic field (Ha = 0), which was studied by Govender (2005). In the case of limit $\Omega \to 0$ (stationary), the critical wave number α_{cr} and critical Rayleigh number $\tilde{R}_{cr}$ approach the values 1 and 3.93 π^2 against the exact values 1 and 4 π^2, respectively. In the existence of vibration, the changeover frequency splitting the synchronous and subharmonic solutions takes place at Ω = 1222.35, in contrast to $\Omega \cong 1225$ of Govender (2005).

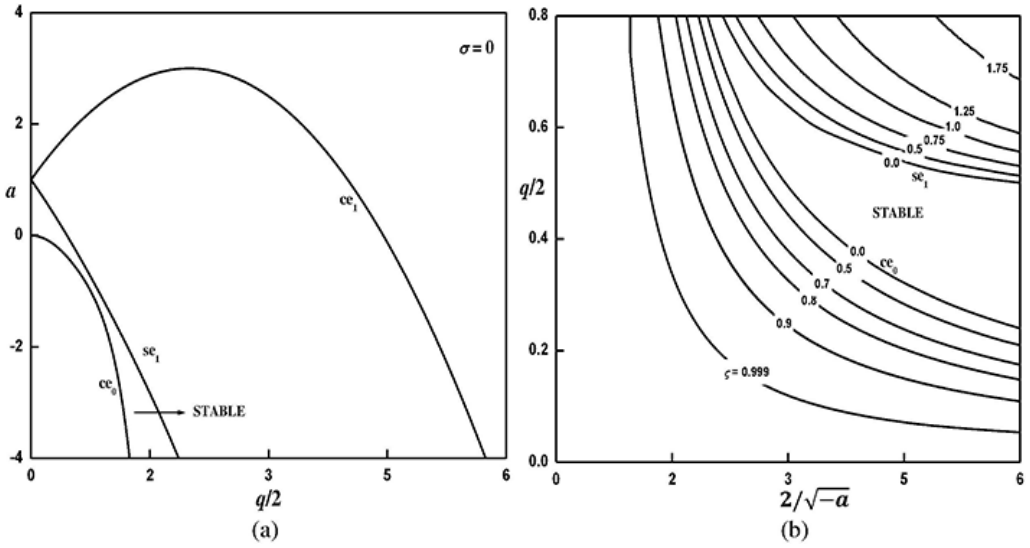

FIG. 2: Stable region as a function a and q: (a) lower order Mathieu's functions depicting stable and unstable regions and (b) stability chart for Mathieu's equation for various values of ς

4. RESULTS AND DISCUSSION

The combined effects of gravity modulation and an externally imposed magnetic field on the onset of convection in an infinite horizontal fluid-saturated anisotropic porous layer which is heated from below is investigated using Brinkman's equation. Based on the prior study and accessibility of necessary data sources, the control parameters are assumed in the following ranges: $10^{-4} \leq \mathrm{Da} \leq 10^{-2}$ and $10^{-1} \leq \xi, \eta \leq 10$. Following Govender (2005), the value of $(\kappa \mathrm{Fr})$ is fixed to be $O(10^{-5})$ corresponding to the solidification of binary liquid metals and $\gamma = O(3)$.

Marginal stability curves for both synchronous and subharmonic solutions are found corresponding to the case of an isotropic porous medium (ξ = η =1) and are graphically shown in Figs. 3(a)–3(c). The characteristic Rayleigh

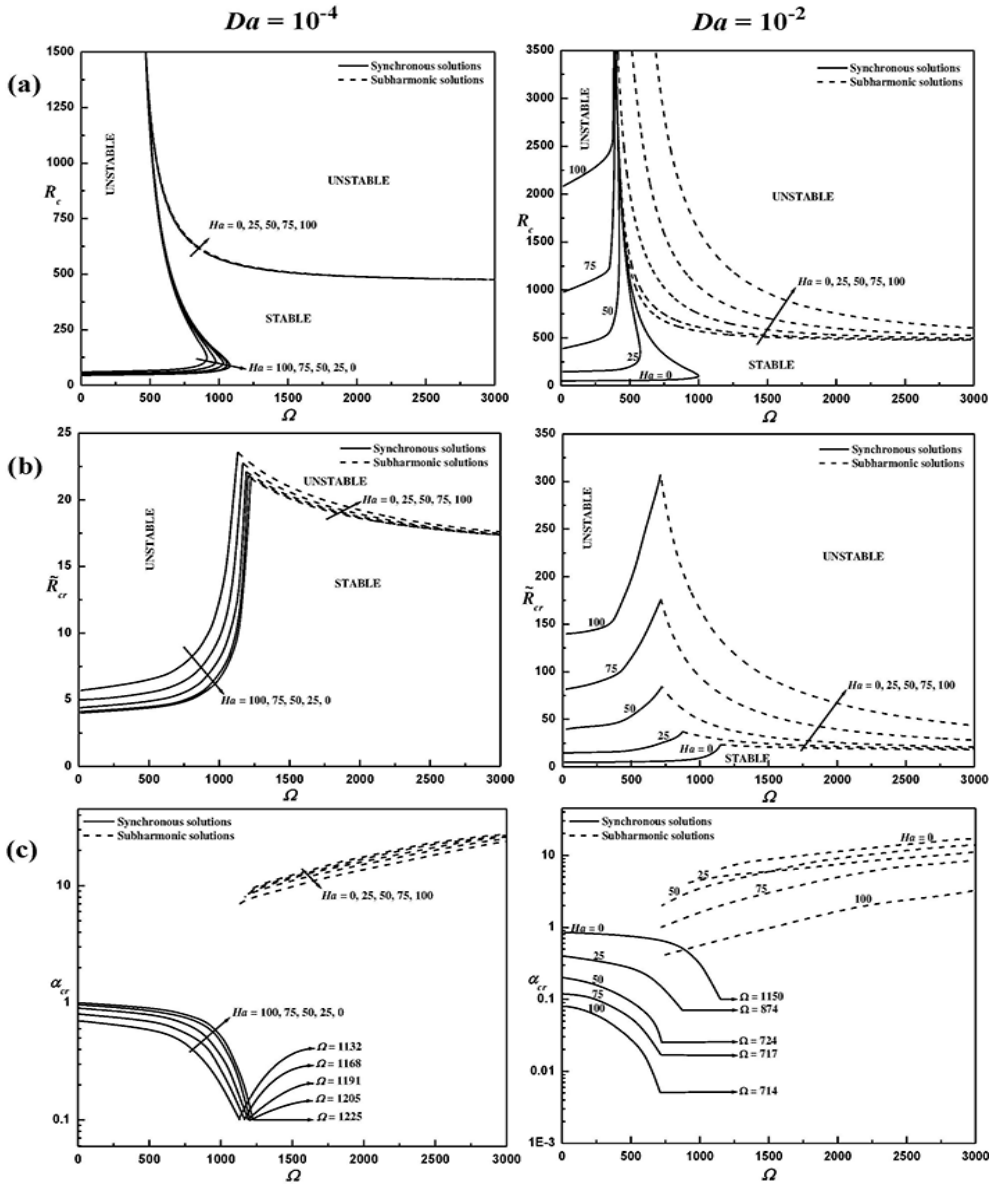

FIG. 3: (a) Characteristic Rayleigh number against frequency for α = 0.5, (b) critical Rayleigh number against frequency, and (c) critical wavenumber against frequency with fixed values of ξ = 1 and η = 1 and different values of Da and Ha

number R_c is plotted against the frequency Ω for various values of Ha and Da when $\alpha = 0.5$ and is shown in Fig. 3(a). It is noted that the region below the curves is stable and the region above them is unstable for both synchronous and subharmonic modes. It is also found that both synchronous and subharmonic solutions are greatly affected by changes in the values of Da from 10^{-4} to 10^{-2}. The critical Rayleigh number $\tilde{R}_{cr}$ and critical wave number α_{cr} against frequency Ω are plotted in Figs. 3(b) and 3(c) for different values of Da and Ha. One should note that the limit $\Omega \to 0$ corresponds to the nonvibrating porous medium, and the critical Rayleigh number tends to the unmodulated value as expected. When Ω is increased from zero, the vibration frequency regulates the onset of convection in the region of synchronous response irrespective of the value of Ha. Moreover, the strength of the applied magnetic field is increased gradually from Ha = 0 to 100 subject to gravity modulation, and the undesirable convection currents are highly suppressed further by the Lorentz force, which ensures the stability of the system. Hence, it is found that the applied magnetic field is more effective in stabilizing the system subject to gravity modulation than the system subject to gravity modulation alone. In the synchronous mode, the stabilizing effect of vibration is weak for lower frequencies and becomes strong for higher frequencies until Ω reaches a certain frequency, beyond which subharmonic mode becomes critical. Further than the crossover point, the effect of increasing the frequency is to slowly destabilize the convection. The transitions occur at different frequencies Ω [see Fig. 3(c)] with respect to Da and Ha and the transition point gets shifted to lower frequencies as the magnetic field strength is increased. However, $\tilde{R}_{cr}$ decreases in the region of subharmonic response and becomes invariant for sufficiently large values of Ω. The corresponding α_{cr} decreases [see Fig. 3(c)] for the synchronous mode and increases for the subharmonic mode with a sudden change at the point of transition as the vibration frequency is increased.

Figures 4(a)–4(c) show the stability characteristics against the vibration frequency Ω for various values of ξ and Ha when Da = 10^{-2}. $\tilde{R}_{cr}$ plotted against Ω in Fig. 4(b) shows that even though an increase in ξ reduces R_c in both synchronous and subharmonic modes, its effect is prominent only in the synchronous mode. The crossover points on the synchronous mode of instability to the subharmonic mode for different values of ξ and Ha is shown in Fig. 4(c). The crossover point becomes shifted to lower frequencies for the strong applied magnetic field; however, ξ shifts the crossover point to a higher frequency region. The corresponding α_{cr} plotted against Ω in Fig. 4(c) shows that strengthening the magnetic field shows a strong reduction in wave number in both synchronous and subharmonic modes. In the same way, the stability characteristics for various values of η and Ha when Da = 10^{-2} is displayed in Figs. 5(a)–5(c). It is evident from Fig. 5(a) that when η increases, R_c also increases for both synchronous and subharmonic modes, supporting the stability of the system. The critical Rayleigh number $\tilde{R}_{cr}$ and critical wave number α_{cr} against frequency Ω are shown in Figs. 5(b) and 5(c) for different values of η. The effect of Ha is found to stabilize the diffusive solution and delay the onset of convection. When comparing Figs. 4 and 5, it is evident that anisotropy in permeability significantly affects the instability compared to that in conductivity with respect to Ha. The transition between the synchronous and subharmonic modes for the different values of η and Ha is shown in Fig. 5(c). It is noted that the amplitude of the disturbance pattern is reduced significantly with increasing η for both synchronous and subharmonic solutions with respect to Ha. In general, the effect of increasing the Ha value for any selected value of Da, ξ, or η is to stabilize the convection corresponding to the synchronous mode and to destabilize the convection in the subharmonic mode. It must be kept in mind that for molten alloy solidification, one is concerned with using low-frequency modulation as well as an external magnetic field to prevent undesired effects such as unfavorable buoyancy-driven convection and sedimentation. Hence, it is expected that the region of synchronous results will be sufficient for use in metal manufacture applications.

5. CONCLUSION

A stability study of gravity modulation on the onset of buoyancy-driven convection in a horizontal porous layer subject to an applied magnetic field has been investigated. The porous domain was assumed to be anisotropic in the mechanical as well as thermal sense along the transverse direction. The investigation was based on the solutions of linearized magnetohydrodynamic Brinkman's equation using the small parameter perturbation technique, and the Boussinesq approximation was used in the field of buoyancy-driven flow. The objective of the current work is to extend the use of Mathieu's functions and stability charts for studying the onset of modulated Rayleigh-Benard convection in a more general porous domain. The results of this study lead to the following conclusions:

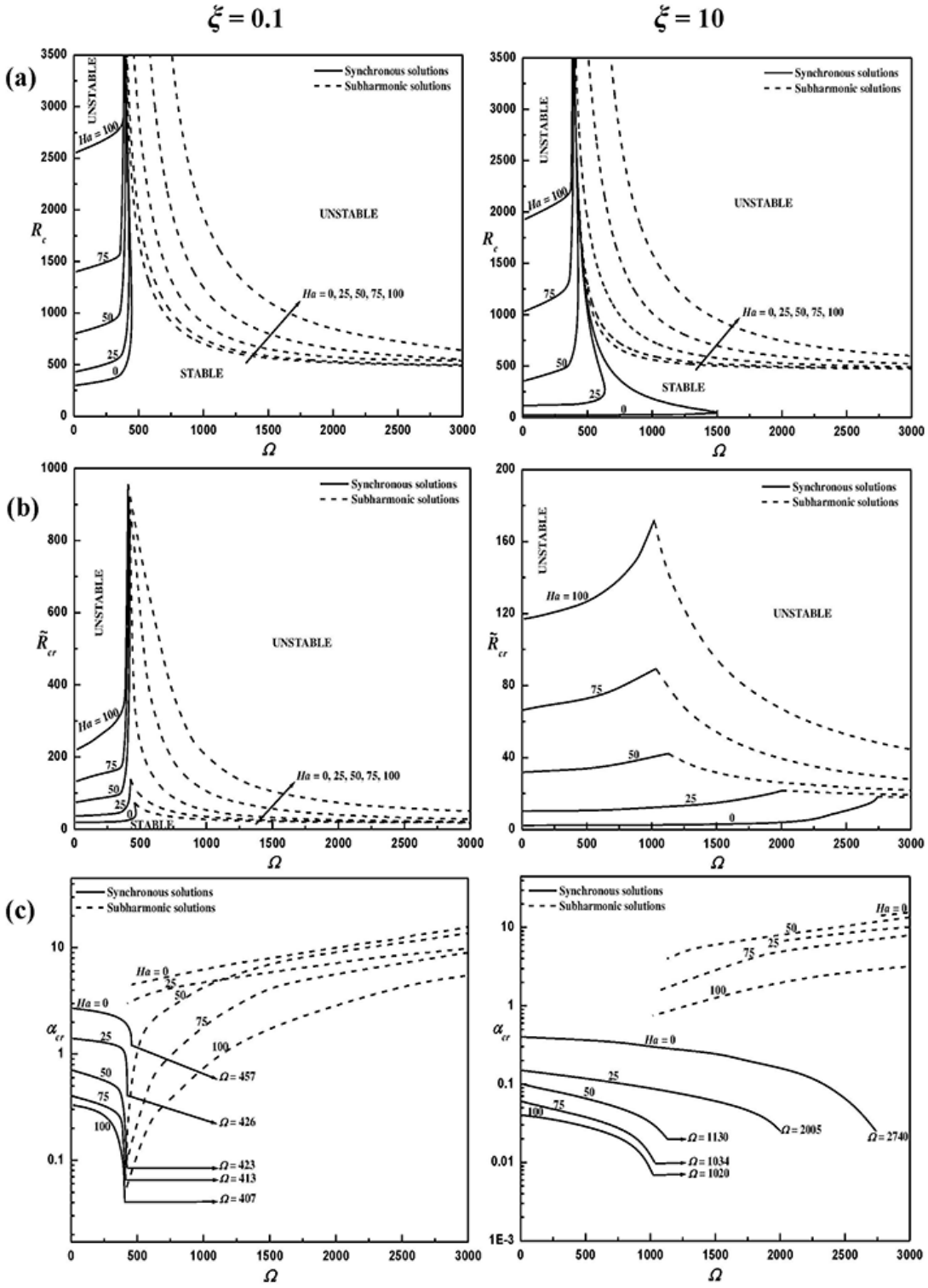

FIG. 4: (a) Characteristic Rayleigh number against frequency for $\alpha = 0.5$, (b) critical Rayleigh number against frequency, and (c) critical wavenumber against frequency with fixed values of $Da = 10^{-2}$ and $\eta = 1$ and different values of ξ, and Ha

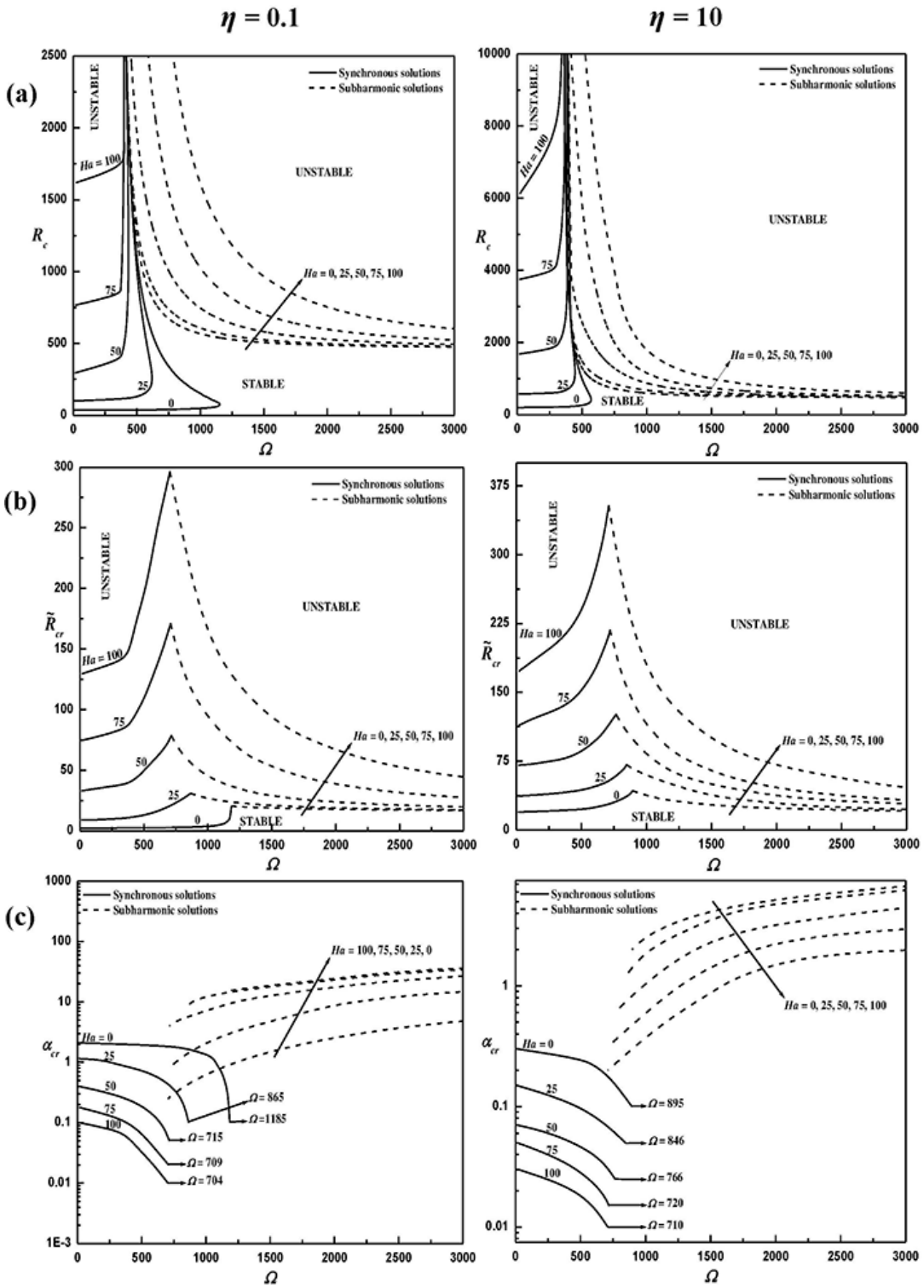

FIG. 5: (a) Characteristic Rayleigh number against frequency for $\alpha = 0.5$, (b) critical Rayleigh number against frequency, and (c) critical wavenumber against frequency with fixed values of $Da = 10^{-2}$ and $\xi = 1$ and different values of η and Ha

(a) The instability mode changes from synchronous to subharmonic as the vibration frequency increases to a certain level. Both the synchronous and subharmonic modes are vastly affected by the non-Darcian effects as well as anisotropies of the porous domain subject to an applied magnetic field.

(b) In the synchronous mode, the stabilizing effect of vibration is weak for lower frequencies and becomes strong for higher frequencies until Ω reaches a certain frequency, beyond which subharmonic mode becomes critical. Further than the crossover point, the effect of increasing the frequency is to slowly destabilize the convection.

(c) The applied magnetic field is more effective in stabilizing the system subject to a modulated gravity field than the system subject to gravity modulation alone, since the undesirable convection currents are highly suppressed further by the Lorentz force, which ensures the stability of the system.

(d) The crossover frequency gets shifted to a lower frequency range for the strong applied magnetic field. The same tendency is noticed when either the medium becomes sparse or the thermal anisotropy parameter becomes large. However, the crossover frequency gets shifted to a higher frequency range when the mechanical anisotropy parameter becomes large.

(e) The critical wave number decreases for the synchronous mode and increases for the subharmonic mode with a sudden change at the point of transition as the vibration frequency is increased.

REFERENCES

Aniss, S., Belhaq, M., and Souhar, M., Effects of a Magnetic Modulation on the Stability of a Magnetic Liquid Layer Heated from above, *J. Heat Transf.*, vol. **123**, no. 3, pp. 428–433, 2001.

Bhadauria, B., Combined Effect of Temperature Modulation and Magnetic Field on the Onset of Convection in an Electrically Conducting-Fluid-Saturated Porous Medium, *J. Heat Transf.*, vol. **130**, no. 5, p. 052601, 2008.

Chamkha, A., Rashad, A., Mansour, M., Armaghani, T., and Ghalambaz, M., Effects of Heat Sink and Source and Entropy Generation on MHD Mixed Convection of a Cu-Water Nanofluid in a Lid-Driven Square Porous Enclosure with Partial Slip, *Phys. Fluids*, vol. **29**, no. 5, p. 052001, 2017.

Chamkha, A., Rashad, A., Armaghani, T., and Mansour, M., Effects of Partial Slip on Entropy Generation and MHD Combined Convection in a Lid-Driven Porous Enclosure Saturated with a Cu-Water Nanofluid, *J. Therm. Anal. Calorim.*, vol. **132**, no. 2, pp. 1291–1306, 2018.

Elder, J.W., Steady Free Convection in a Porous Medium Heated from below, *J. Fluid Mech.*, vol. **27**, no. 1, pp. 29–48, 1967.

Gershuni, G., Zhukhovitskii, E., and Iurkov, I.S., On Convective Stability in the Presence of Periodically Varying Parameter, *J. Appl. Math. Mech.*, vol. **34**, no. 3, pp. 442–452, 1970.

Govender, S., Linear Stability and Convection in a Gravity Modulated Porous Layer Heated from below: Transition from Synchronous to Subharmonic Solutions, *Transp. Porous Media*, vol. **59**, no. 2, pp. 227–238, 2005.

Govender, S., On the Effect of Anisotropy on the Stability of Convection in Rotating Porous Media, *Transp. Porous Media*, vol. **64**, no. 3, pp. 413–422, 2006.

Gresho, P. and Sani, R., The Effects of Gravity Modulation on the Stability of a Heated Fluid Layer, *J. Fluid Mech.*, vol. **40**, no. 4, pp. 783–806, 1970.

Horton, C. and Rogers, Jr., F., Convection Currents in a Porous Medium, *J. Appl. Phys.*, vol. **16**, no. 6, pp. 367–370, 1945.

Ingham, D.B. and Pop, I., *Transport Phenomena in Porous Media*, Amsterdam: Elsevier, 1998.

Katto, Y. and Masuoka, T., Criterion for the Onset of Convective Flow in a Fluid in a Porous Medium, *Int. J. Heat Mass Transf.*, vol. **10**, no. 3, pp. 297–309, 1967.

Lapwood, E., Convection of a Fluid in a Porous Medium, *Math. Proc. Cambridge Philosoph. Soc.*, vol. **44**, pp. 508–521, 1948.

Li, B., Stability of Modulated-Gravity-Induced Thermal Convection in Magnetic Fields, *Phys. Rev. E*, vol. **63**, no. 4, p. 041508, 2001.

Mahabaleswar, U., Combined Effect of Temperature and Gravity Modulations on the Onset of Magneto-Convection in Weak Electrically Conducting Micropolar Liquids, *Int. J. Eng. Sci.*, vol. **45**, nos. 2-8, pp. 525–540, 2007.

Malashetty, M. and Padmavathi, V., Effect of Gravity Modulation on the Onset of Convection in a Fluid and Porous Layer, *Int. J. Eng. Sci.*, vol. **35**, no. 9, pp. 829–840, 1997.

Malashetty, M. and Swamy, M., Effect of Rotation on the Onset of Thermal Convection in a Sparsely Packed Porous Layer Using a Thermal Non-Equilibrium Model, *Int. J. Heat Mass Transf.*, vol. **53**, nos. 15-16, pp. 3088–3101, 2010.

McLachlan, N., *Theory and Application of Mathieu Functions*, New York: Dover, 1964.

Nield, D.A. and Bejan, A., *Convection in Porous Media*, vol. **3**, Berlin: Springer, 2006.

Purusothaman, A., Investigation of Natural Convection Heat Transfer Performance of the QFN-PCB Electronic Module by Using Nanofluid for Power Electronics Cooling Applications, *Adv. Powder Technol.*, vol. **29**, no. 4, pp. 996–1004, 2018.

Purusothaman, A., Nithyadevi, N., Oztop, H., Divya, V., and Al-Salem, K., Three Dimensional Numerical Analysis of Natural Convection Cooling with an Array of Discrete Heaters Embedded in Nanofluid Filled Enclosure, *Adv. Powder Technol.*, vol. **27**, no. 1, pp. 268–280, 2016a.

Purusothaman, A., Oztop, H., Nithyadevi, N., and Abu-Hamdeh, N.H., 3D Natural Convection in a Cubical Cavity with a Thermally Active Heater under the Presence of an External Magnetic Field, *Comput. Fluids*, vol. **128**, pp. 30–40, 2016b.

Rashad, A., Armaghani, T., Chamkha, A., and Mansour, M., Entropy Generation and MHD Natural Convection of a Nanofluid in an Inclined Square Porous Cavity: Effects of a Heat Sink and Source Size and Location, *Chinese J. Phys.*, vol. **56**, no. 1, pp. 193–211, 2018.

Saravanan, S. and Purusothaman, A., Floquet Instability of a Gravity Modulated Rayleigh–Benard Problem in an Anisotropic Porous Medium, *Int. J. Thermal Sci.*, vol. **48**, no. 11, pp. 2085–2091, 2009.

Siddheshwar, P., Bhadauria, B., Mishra, P., and Srivastava, A.K., Study of Heat Transport by Stationary Magneto-Convection in a Newtonian Liquid under Temperature or Gravity Modulation Using Ginzburg–Landau Model, *Int. J. Non-Linear Mech.*, vol. **47**, no. 5, pp. 418–425, 2012.

Srivastava, A.K. and Bhadauria, B., Linear Stability of Solutal Convection in a Mushy Layer Subjected to Gravity Modulation, *Commun. Nonlinear Sci. Numer. Simul.*, vol. **16**, no. 9, pp. 3548–3558, 2011.

Vafai, K., *Handbook of Porous Media*, New York: Taylor and Francis Group, 2005.